

This dissertation has been 64-8880
microfilmed exactly as received

LANG, Wayne Wilson, 1936-
CHARGE-CHANGING COLLISIONS OF
OXYGEN IONS IN THE 50-400 KILOVOLT
KINETIC ENERGY RANGE.

The University of Nebraska, Ph.D., 1964
Physics, general

University Microfilms, Inc., Ann Arbor, Michigan

Copyright by

Wayne Wilson Lang

1964

PREVIEW

CHARGE-CHANGING COLLISIONS OF OXYGEN IONS
IN THE 50-400 KILOVOLT KINETIC ENERGY RANGE

by
Wilson
Wayne Lang

A THESIS
Presented to the Faculty of
The Graduate College in the University of Nebraska
In Partial Fulfillment of Requirements
For the Degree of Doctor of Philosophy
Department of Physics

Under the Supervision of Dr. Theodore Jorgensen, Jr.

Lincoln, Nebraska

August 1963

TITLE

Charge-changing Collisions of Oxygen Ions in the

50-400 Kilovolt Kinetic Energy Range

BY

Wayne W. Lang

APPROVED

DATE

Theodore Jorgensen, Jr.

Oct. 26, 1963

M. A. Basoco

Oct. 26, 1963

E. J. Zimmerman

Oct. 26, 1963

John J. Scholz

Oct. 26, 1963

Edgar A. Pearlstein

Oct. 26, 1963

SUPERVISORY COMMITTEE

GRADUATE COLLEGE

UNIVERSITY OF NEBRASKA

ACKNOWLEDGEMENTS

I would like to thank Professor Jorgensen for suggesting this experiment and helping and encouraging me during this work.

My sincere appreciation also to Bill Fraser for programing computations done at the Nebraska Computing Center; to Mr. J. Helser, Mr. D. Fuehring, and Mr. E. Brooks for the construction of the apparatus; and to my wife Phyllis for typing the manuscript.

It is a pleasure to acknowledge the support of a National Science Foundation Cooperative Fellowship during three of my years as a graduate student. The research was supported in part by the United States Atomic Energy Commission.

TABLE OF CONTENTS

List of Figures	ii
List of Tables	iv
I. Introduction	1
II. Magnetic Analysis of the Ion Beam	8
III. Measurement of the Equilibrated Beam Fractions	11
A. Experimental Apparatus	
1. Converter Cell	
2. Magnetic Separation Chamber	
3. Neutral Detector	
4. Charged Particle Detector	
5. Electrometers for Current Measurements	
B. Experimental Procedure	
1. Method of Taking Data	
2. Experimental Tests of Apparatus	
3. Calculation of Beam Fractions from the Data	
IV. Measurement of Total Cross Sections	27
A. Experimental Apparatus	
B. Experimental Procedure	
1. Neutral Component Attenuation Measurements	
2. Charged Components Attenuation Measurements	
C. Calculation of Total Cross Sections from Data	
V. Results	40
A. Equilibrium Beam Fractions	
B. Total Cross Sections	
VI. Deductions from Experimental Results	52
A. Values of Individual Cross Sections	
B. Sample Deduction of Individual Cross Sections for Oxygen Ions with 100 keV energy in H ₂ Target Gas	
C. Differential Equations of Beam Growth	
VII. Discussion of the Results	75
A. Electron Loss Cross Sections	
B. Electron Capture Cross Sections	
VIII. Conclusion	87
References	88

LIST OF FIGURES

<u>Figures</u>	<u>Page</u>
1. Schematic Diagram of Beam Fraction Apparatus.	2
2. Schematic Diagram of Beam Attenuation Apparatus	4
3. Magnetic Analysis of Beam from Accelerator	9
4. Diagram of Converter Cell	12
5. Diagram of Beam Component Separation Chamber for Beam Fraction Measurements	13
6. Neutral Detector.	15
7. Charged Particle Detector	17
8. Growth of Beam Components from Originally Pure O ⁺ Beam	22
9. Profile of Beam Current in Charged Particle Detector Positioned at 30° Port	24
10. Secondary Electrons per Oxygen Ion Incident on Platinum (300° C).	26
11. Attenuation Chamber	29
12. Beam Profile at 15° Port with Attenuation Chamber Exit Opening of .125" -- 200 keV	36
13. Beam Profile at 30° Port with Attenuation Chamber Exit Opening of .025" -- 200 keV	37
14. Equilibrium Fractions, $F_{i\infty}$ Oxygen Ions in Hydrogen Target Gas	43
15. Equilibrium Fractions, $F_{i\infty}$ Oxygen Ions in Helium Target Gas	44
16. Equilibrium Fractions, $F_{i\infty}$ Oxygen Ions in Oxygen Target Gas	45
17. Total Cross Sections $\sum \sigma_{if}$ for Oxygen Ions in Target Gas of Hydrogen	48
18. Total Cross Sections $\sum \sigma_{if}$ for Oxygen Ions in Target Gas of Helium	49

FiguresPage

19. Total Cross Sections $\sum \sigma_{if}$ for Oxygen Ions in Target Gas of Oxygen	50
20. Cross Sections Oxygen Ions in Hydrogen Target Gas	67
21. Cross Sections Oxygen Ions in Helium Target Gas .	68
22. Cross Sections Oxygen Ions in Oxygen Target Gas .	69
23. Growth of Beam Components from Originally Pure O^+ Beam (200 keV- H_2 Gas)	74

LIST OF TABLES

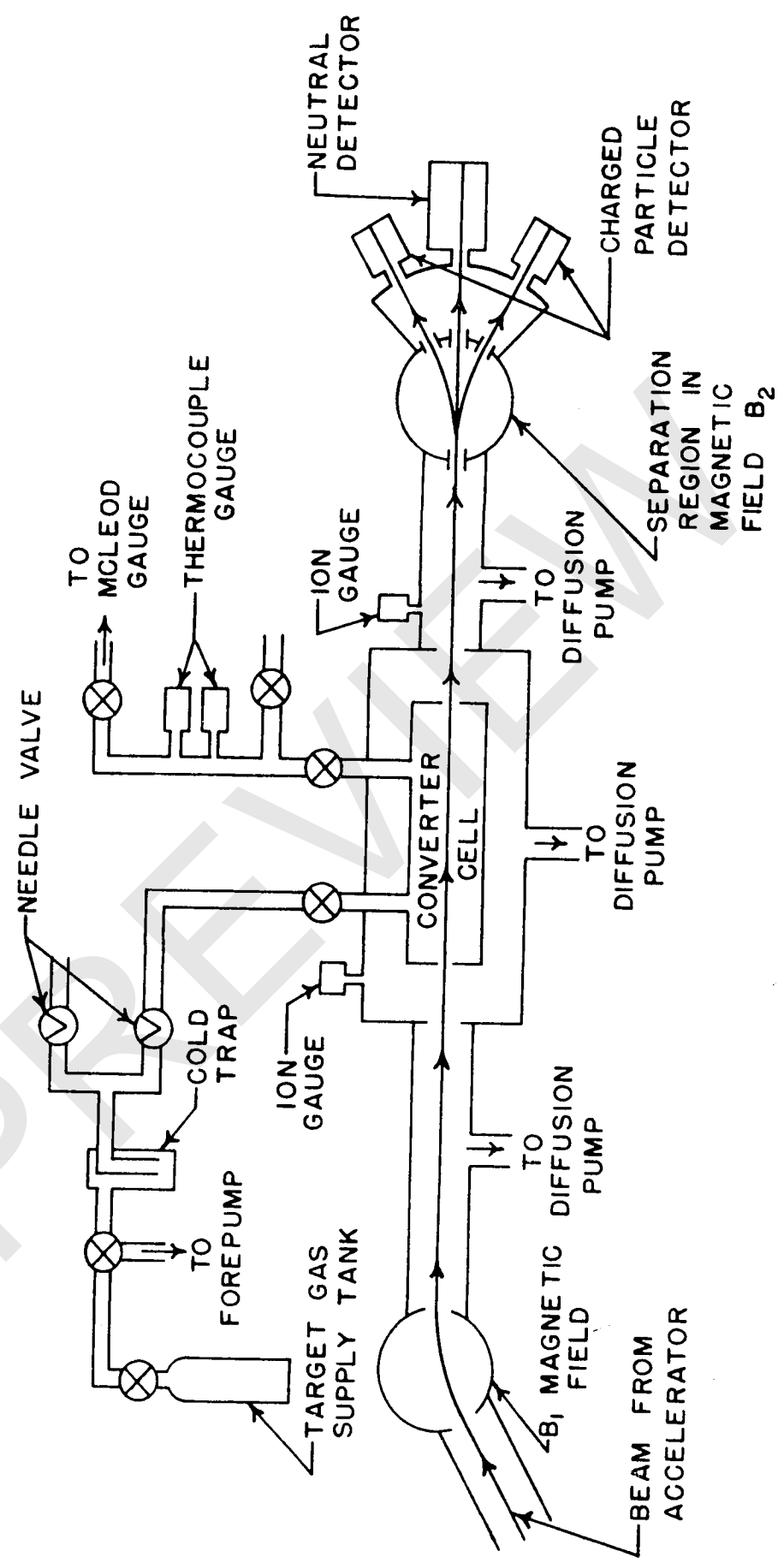
<u>Tables</u>	<u>Page</u>
I. Equilibrium Beam Fractions	41
II. Total Cross Section Sums.	47
III. Comparison of a Few Trial Total Cross Section Sums for Hydrogen Ions with Those of Other Investigators	51
IV. Internal Consistency Identities	62
V. Deduced Individual Cross Sections (Hydrogen Target Gas)	63
VI. Deduced Individual Cross Sections (Helium Target Gas)	64
VII. Deduced Individual Cross Sections (Oxygen Target Gas)	65
VIII. Estimated Ratios of Double to Single Electron Captures and Losses Based on Helium and Hydrogen Ion Data.	65
IX. Predicted Velocity of Cross Section Maxima	76
X. Electron Loss Cross Section σ_{01} at an Ion Energy of 50 keV	76
XI. Comparison of Electron Loss Cross Sections for Oxygen Ions from this Experiment with those of Dmitriev at an Ion Velocity of 25×10^7 cm/sec	81
XII. Electron Capture Cross Sections σ_{01} at an Ion Energy of 50 keV	81
XIII. Comparison of Electron Capture Cross Sections for Oxygen Ions for this Experiment with those of Nikoleav at an Ion Velocity of 25×10^7 cm/sec	84
XIV. Comparison of the p Values of the Present Experiment with those of Nikolaev for Capture Cross Sections	86

I. INTRODUCTION

A beam of O^+ ions is prepared by using a radio frequency source containing O_2 gas and accelerating the singly charged oxygen ion electrostatically to the desired kinetic energy. When such an ion beam enters a gas-containing chamber, hereafter called the converter cell, inelastic collisions take place in which the charge of the moving ions is changed, by capture or loss of one or more electrons. The newly-formed beam constituents in turn suffer such charge-changing collisions. After a sufficient path length in the converter cell, the beam has come to charge equilibrium, and the fractions $F_{l\infty}$ of the various charged types present is a function only of the velocity of the beam and the nature of the converter gas. Let l represent the positive charge on the beam constituent in units of the electronic charge. In the present experiments the fractions $F_{l\infty}$ with $l = -1, 0, 1, 2,$ and 3 were measured in the gases H_2 , He, and O_2 . A schematic diagram of this part of the experiment is shown in Figure 1.

A second aspect of the experiments dealt with the measurement of the collision cross sections for such charge changing events. The method of measurement indicated only that the charge of the moving oxygen ion had been changed in the collision; it did not in itself indicate whether the event had been electron loss or capture, either single or multiple. Therefore, the quantity measured is indicated as $\sum_f \sigma_{lf}$, l referring, as above, to the ionic charge before

Figure 1.



SCHEMATIC DIAGRAM OF BEAM FRACTION APPARATUS

the event, and \underline{f} the charge after the event, and σ_{if} is the cross section for the charge exchange process. By using the various charged constituents emerging from the converter cell, $\sum_f \sigma_{if}$ for $\underline{i} = -1, 0, 1$, and 2 were measured in target gases of H_2 , He, and O_2 . A schematic diagram of this second part of the experiment is shown in Figure 2.

We can see from Figures 1 and 2 that the apparatus for the two parts of the experiment is the same except for the region of the magnetic field B_2 . In the first part of the experiment, the B_2 field region was maintained at a high vacuum while in the second part the B_2 field region had to hold target gases.

In the energy range of this experiment, oxygen ions of positive charge value greater than two were shown to be a very small fraction of the beam. Therefore, the differential equations can be solved by ignoring these higher charge states with introduction of very little error.

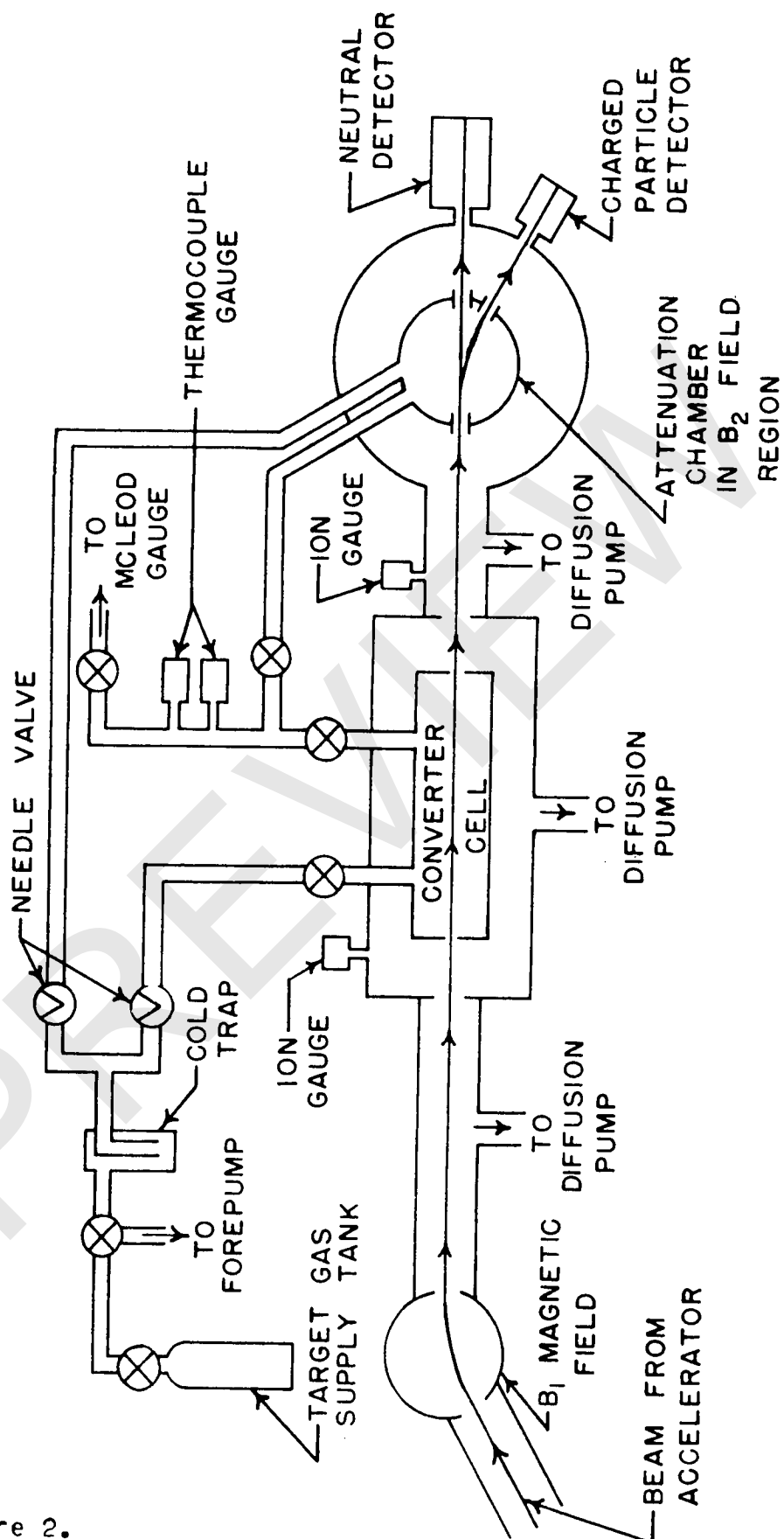
There are four differential equations (three of which are independent) which give the rate of change of the fraction of any charge component. Written in a form such that π represents the number of gas molecules per cm^2 in the path of the beam, the differential equations are:

$$\frac{dF_{\underline{i}}}{d\pi} = \sum_i F_i \sigma_{i\underline{i}} - F_{\underline{i}} \sum_f \sigma_{if}$$

$$\frac{dF_0}{d\pi} = \sum_i F_i \sigma_{i0} - F_0 \sum_f \sigma_{0f}$$

$$\frac{dF_1}{d\pi} = \sum_i F_i \sigma_{i1} - F_1 \sum_f \sigma_{1f}$$

Figure 2.



SCHEMATIC DIAGRAM OF BEAM ATTENUATION APPARATUS

$$\frac{dF_2}{dt} = \sum_i F_i \sigma_{i2} - F_2 \sum_f \sigma_{2f}$$

The above equations simply state that the rate of increase in a given fraction is equal to the number of atoms changing charge into the charge state minus those changing charge out of the charge state. If the derivatives are set equal to zero, corresponding to the condition of the equilibrated beam, then the following equations result:

$$\sum_i F_{i\infty} \sigma_{i1} = F_{1\infty} \sum_f \sigma_{1f} \quad (1)$$

$$\sum_i F_{i\infty} \sigma_{i0} = F_{0\infty} \sum_f \sigma_{0f} \quad (2)$$

$$\sum_f F_{f\infty} \sigma_{f1} = F_{1\infty} \sum_f \sigma_{1f} \quad (3)$$

$$\sum_i F_{i\infty} \sigma_{i2} = F_{2\infty} \sum_f \sigma_{2f} \quad (4)$$

As an example let us examine Eq. (1). If $\sum_f \sigma_{1f}$ is measured along with $F_{0\infty}$, $F_{1\infty}$, $F_{1\infty}$, and $F_{2\infty}$, then upon solving for σ_{01} we have:

$$\sigma_{01} = \frac{F_{1\infty} \sum_f \sigma_{1f} - [F_{1\infty} \sigma_{11} + F_{2\infty} \sigma_{21}]}{F_{0\infty}}$$

The terms inside the brackets involve double and triple electron capture cross sections that are small compared to those of single electron capture. If the terms in the brackets are less than 10% of $F_{1\infty} \sum_f \sigma_{1f}$, then to within the experimental error of 10%:

$$\sigma_{01} = \frac{F_{1\infty} \sum_f \sigma_{1f}}{F_{0\infty}}$$

We will see later that certain estimates can be applied to the terms in the brackets that will result in a better evaluation of the single electron capture. Similar analysis

can be applied to Eqs. (2), (3), and (4). This discussion demonstrates the motivation for making measurements of

$\sum_f \sigma_{if}$ and the equilibrium fractions.

Experimental measurements of this type have been carried out by many investigators. Cross section measurements for hydrogen and helium ions have been done by Stier and Barnett,¹ Montague,² Kanner,³ Whittier,⁴ Allison,⁵ and others. Helium and hydrogen ion experiments prior to 1958 are discussed extensively in a review article by Allison.⁶ Allison⁷ has made measurements on the lithium ions, with experimental procedures very similar to those applied to the present experiment. Fogel⁸ has used another method of making these cross section measurements and his results are compared with those of the present experiment.

Dmitriev^{10,11} and Nikolaev^{12,13} have made electron loss and capture cross section measurements using a cyclotron for ion acceleration. The low energy limit of their experiments is only slightly above the high energy limit of the present experiment. They do not use oxygen ions, so a comparison is made with their nitrogen ion data.

There is presently no general theory for the behavior of charge-changing cross sections. The relationships that exist between cross sections, ion velocity, binding energy of the lost or captured electron, and Z number of the target gas are of an empirical nature for all but the simplest ion-atom pairs. Electron loss cross sections all pass through maxima, and the ion velocities, at which these maxima occur, increase as the ionization potential of the

lost electron increases. This will be discussed in Section VII, and the data of this experiment will be tested with this relation.

Quantum mechanical calculations are very complicated for even the simple cases of hydrogen and helium ions and are, in general, not in good agreement with this experiment. In order to test a general theory that applies to charge-changing cross sections for all ion-atom pairs, experimental data for numerous ion-atom combinations over wide velocity ranges must be accumulated.

Then, the purpose of this experiment is twofold: first, to determine if consistent single electron capture and loss cross sections can be deduced from measurements of equilibrium fractions and total cross section sums; and second, to add these deduced cross sections to the growing body of knowledge about this very complicated field of charge-changing collisions.

II. MAGNETIC ANALYSIS ON THE ION BEAM

In all the measurements, the ion beam leaving the accelerator tube was magnetically analyzed before passing into the converter cell (see Fig. 1). A magnetic analysis of the beam revealed the presence of many ions in the magnetic field range where the O^+ ion was expected to be found. Therefore, a careful mass spectrum analysis was carried out in order to determine, definitely, which of these was indeed the O^+ ion.

Let e be the charge and m the mass of an ion, V the accelerator potential, B the field of the analyzer magnet and R the radius of curvature of the ion in this field. The relation that applies is as follows:

$$m/e = \frac{1/2 R^2}{V} B^2 = (\text{constant}) B^2.$$

The B field was directly proportional to the magnet current which was measured with an ammeter.

The result of the analysis is shown in Figure 3 with the quantity B^2 in arbitrary units. The solid lines are displaced away from the dotted lines only for illustrative purposes. The graph shows only the height of the spectrum peaks. The half-widths were very narrow, being only about one-tenth of a m/e unit wide. This spectrum shows conclusively that the ion which is second in intensity when the ion source is filled with air and then greatly increases in intensity when oxygen is introduced into the source is the O^+ ion.

The O^+ ion was assigned a m/e ratio of 16 and the scale

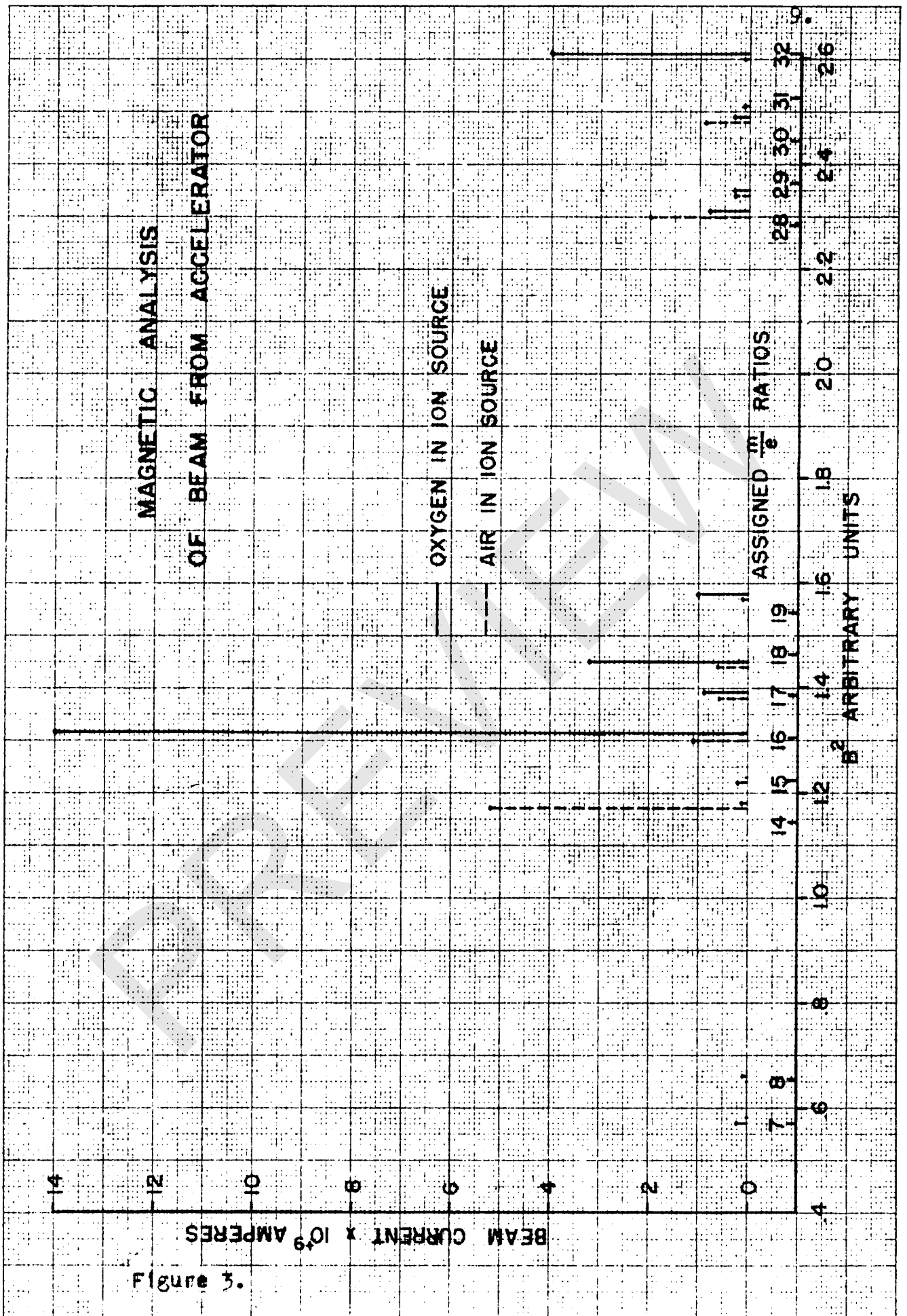


Figure 3.

of m/e ratios was plotted out along the B^2 axis. In this way it was determined that the beam coming into the apparatus at an m/e ratio of 8 can be O^{++} or possibly NH_2^{++} . Therefore, the magnetic analyzer was set at this value when the O^{++} double energy ion was desired. By carefully keeping nitrogen and hydrogen out of the ion source, the possibility that a significant fraction of the beam was NH_2^{++} was removed. We note that the m/e values corresponding to the N_2^+ and O_2^+ molecular ions are at 28 and 32, which are their proper positions in the spectrum.

The peaks of the various ions in the spectrum do not fall exactly on the integer values of the assigned m/e ratios because of hysteresis effects in the magnet.

III. MEASUREMENT OF THE EQUILIBRATED BEAM FRACTIONS $F_{1\infty}$

A. Experimental Apparatus

1. Converter Cell

The design of the converter cell is shown in Figure 4. The cell is comprised of a tube 50 cm. long, 2" in diameter, with beam entrance and exit apertures 0.040" in diameter. A large volume diffusion pump removes the gas that appears between the two diaphragms at either end of the converter cell, a small volume diffusion pump pumps from the region between the converter cell and the analyser magnet and a third diffusion pump keeps the pressure at about 10^{-5} mm. of mercury or lower in the region where the beam components are separated by the magnetic field B_2 .

A small pipe leads from the needle valve into the converter cell through which the target gas is admitted. Likewise, a 0.5" diameter pipe leads from the converter cell to a pair of thermocouple gauges which are in turn connected to a McLeod gauge. The thermocouple gauges, calibrated with the McLeod gauge, measure the pressure in the converter cell.

2. Magnetic Separation Chamber

The design of the magnetic separation chamber is shown in Figure 5. Because of the large magnetic field necessary to deflect the relatively heavy oxygen ions and the desire to use an electromagnet previously constructed for hydrogen

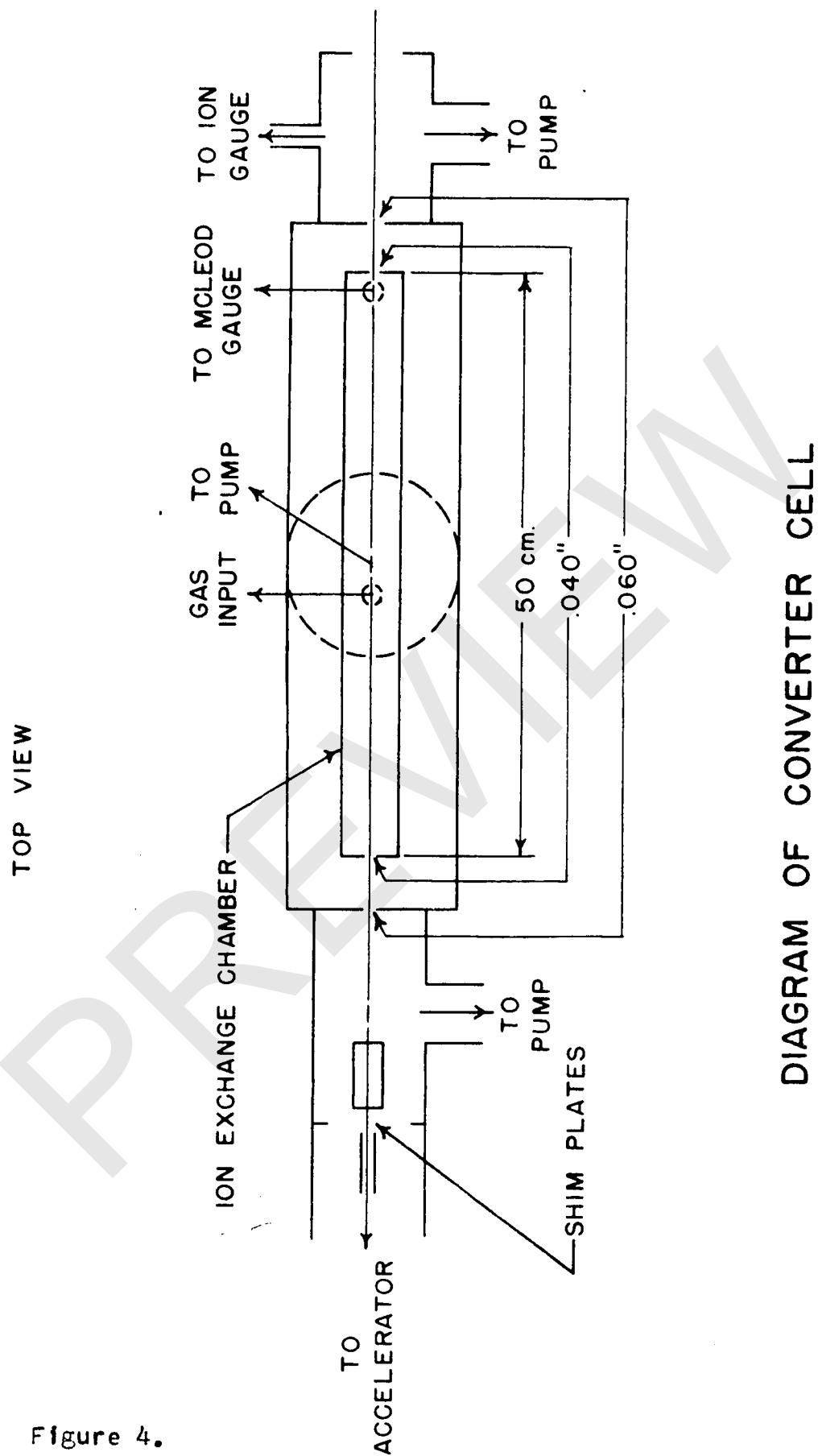


Figure 4.

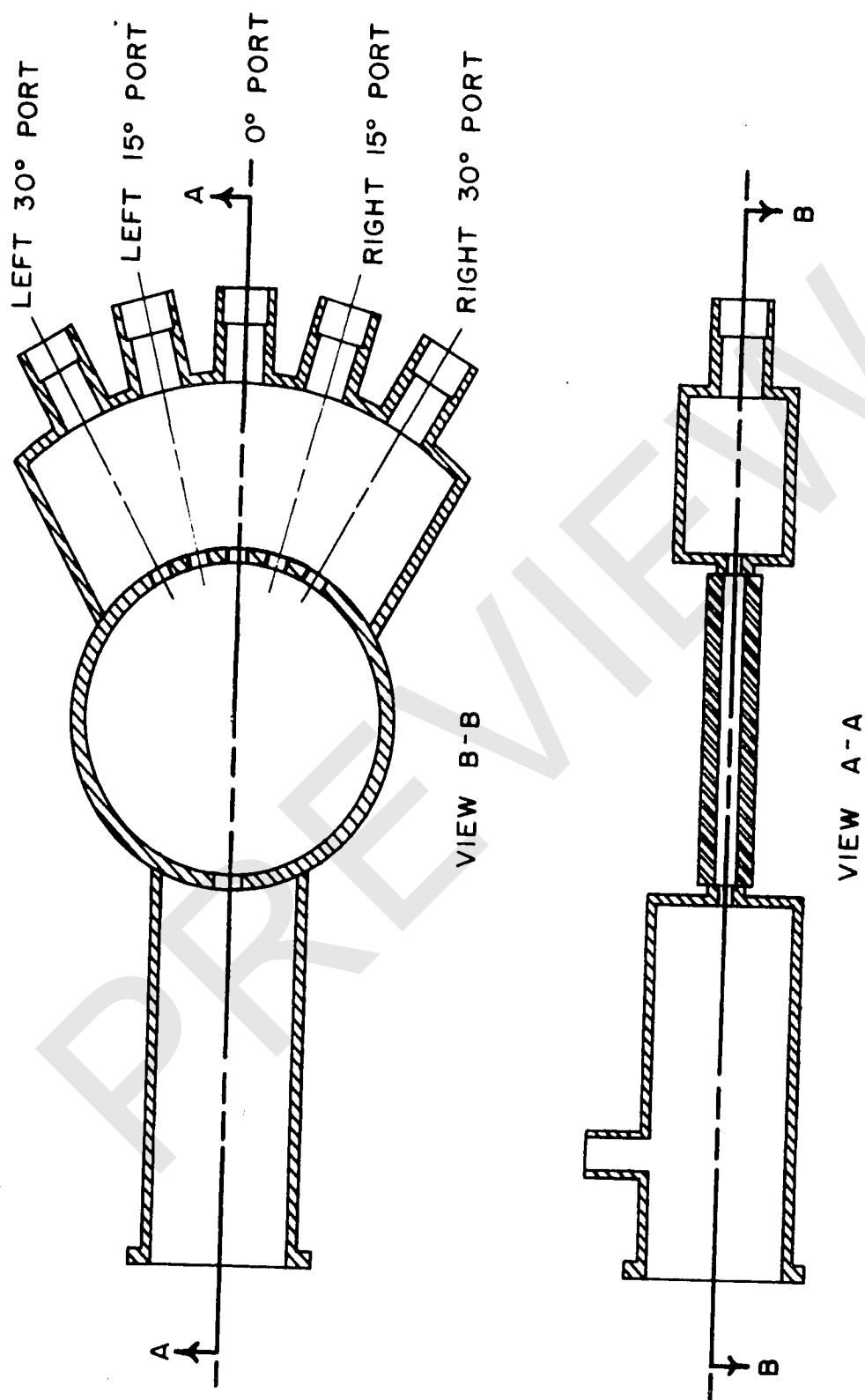


Figure 5.

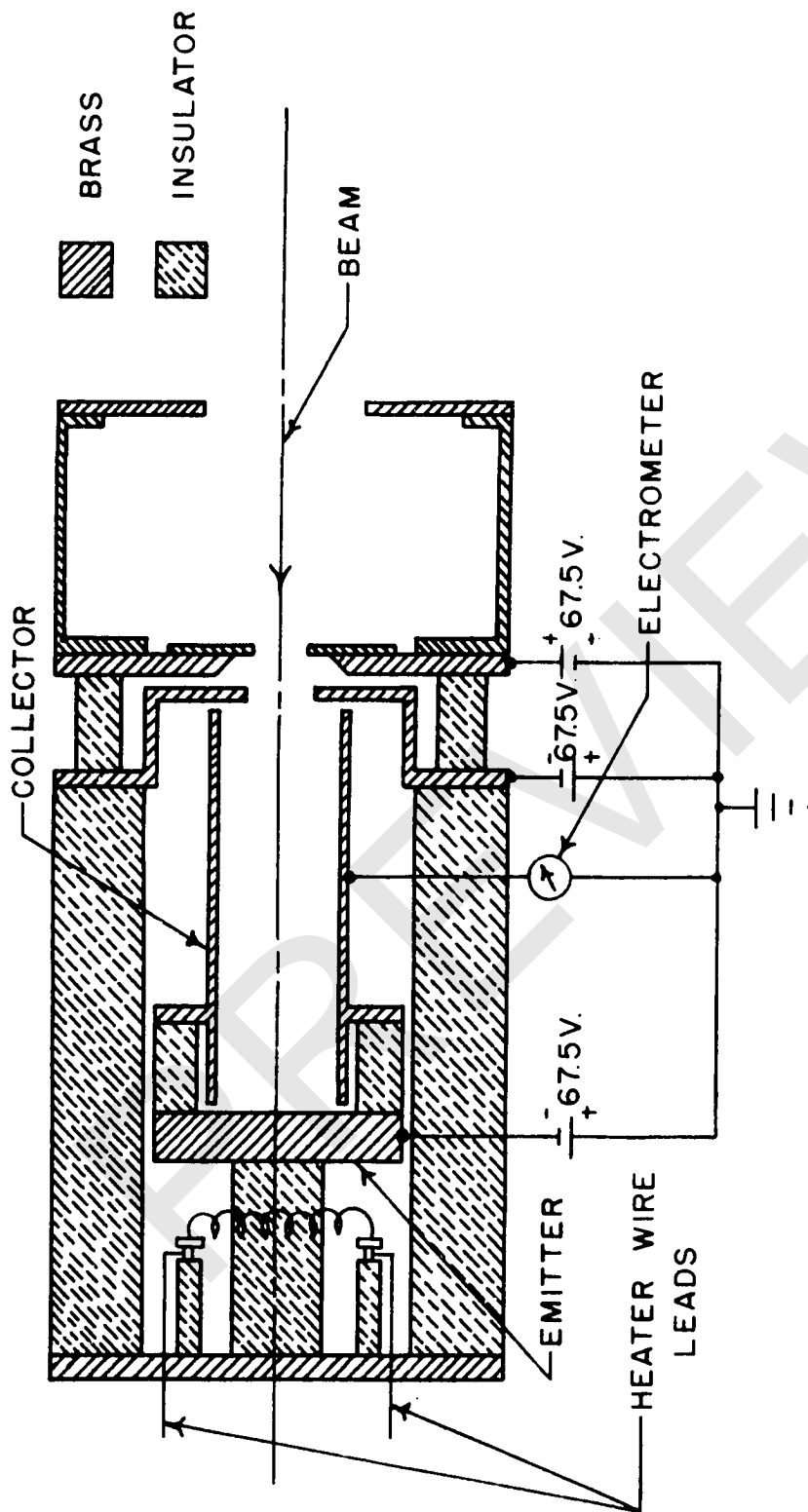
DIAGRAM OF BEAM COMPONENT SEPARATION CHAMBER
FOR BEAM FRACTION MEASUREMENTS

and helium ion experiments, it was necessary to make the gap between the pole faces of the magnet as small as practicable. Therefore, the flat circular portion of the chamber that must fit in between the pole faces of the magnet should not be too thick, yet must have sufficient room inside to pass the beam through it without striking the chamber walls. It was determined that at least 0.35" inside chamber dimension was needed to prevent interference with the beam and that the outside dimension could not be greater than 0.5" and still have enough magnetic field strength to deflect 400 keV oxygen ions through an angle of 30° . Therefore, it was decided to make the walls of the chamber in the magnetic field region of 0.25" steel and to use the steel both as the pole faces of the magnet and also as the vacuum chamber walls. This design proved to be very satisfactory.

The magnetic separation chamber is equipped with a zero degree port to which the neutral detector is attached, two 15° and two 30° ports, on the left and right side, for the attachment of the charged particle detectors. In the course of the experiment the ports which did not have a detector attached were plugged with rubber stoppers.

3. Neutral Detector

The details of the secondary electron detector used in the measurement of the neutral portion of the beam are shown in Figure 6. The beam strikes the target, made of platinum, which gives off secondary electrons which are collected by



NEUTRAL DETECTOR

Figure 6.